

## Solar Radiation on a Catenary Collector

M. Crutchik  
*Tel-Aviv University*  
*Tel-Aviv, Israel*

and

J. Appelbaum  
*Lewis Research Center*  
*Cleveland, Ohio*

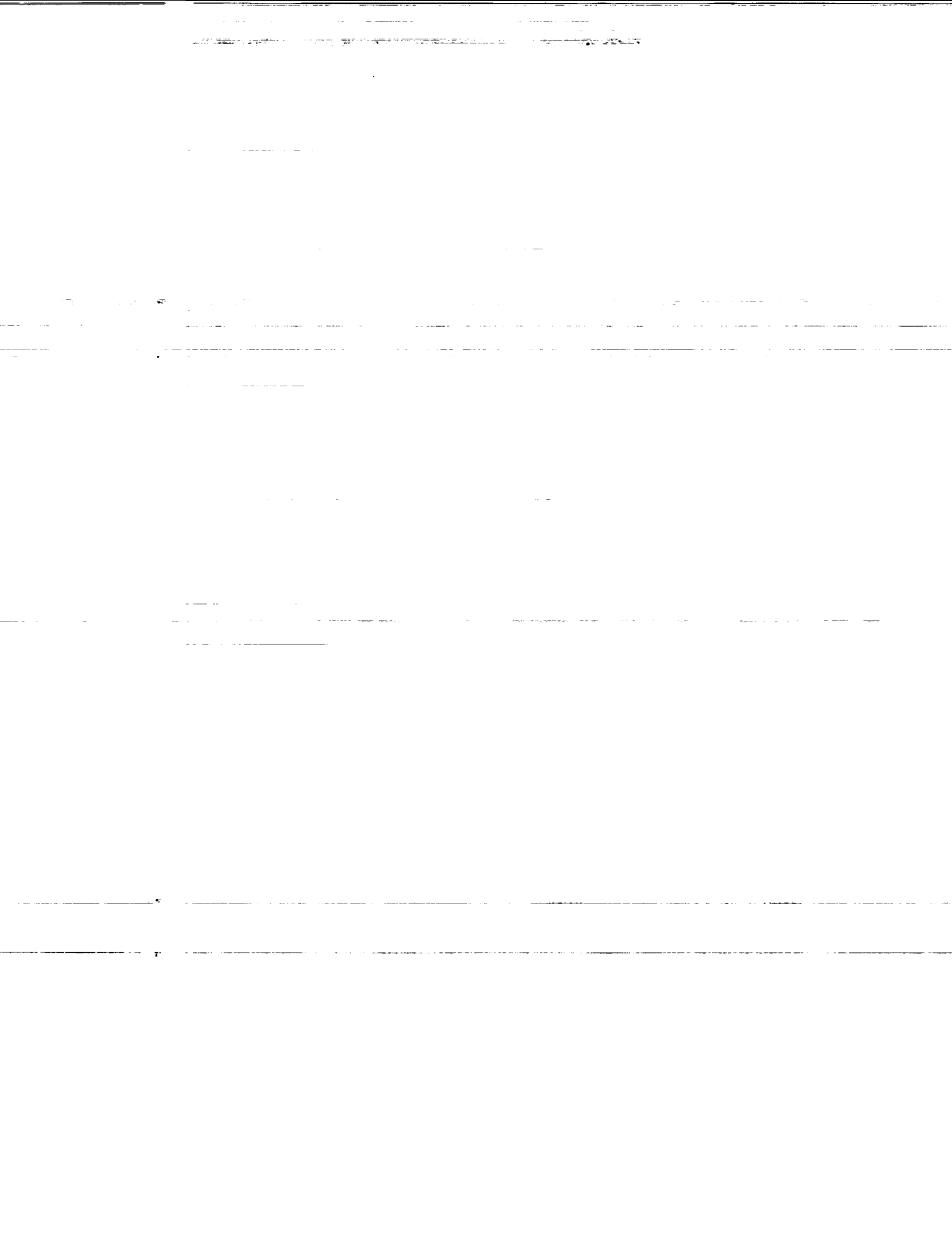
**NASA**

(NASA-TM-105751) SOLAR RADIATION  
ON A CATENARY COLLECTOR (NASA)  
32 p

N92-32243

Unclas

G3/33 0110079



## SOLAR RADIATION ON A CATENARY COLLECTOR

M. Crutchik

Faculty of Engineering

Tel-Aviv University

Tel-Aviv 69978, Israel

J. Appelbaum<sup>†</sup>

National Aeronautics and

Space Administration

Lewis Research Center,

Cleveland, OH 44135

### Abstract

A tent-shaped structure with a flexible photovoltaic blanket acting as a catenary collector is presented. The shadow cast by one side of the collector on the other side producing a self shading effect is analysed. The direct beam, the diffuse and the albedo radiation on the collector are determined. An example is given for the insolation on the collector operating on Mars surface for the location of Viking Lander 1 (VL1).

---

<sup>†</sup>Current address: Tel-Aviv University, Faculty of Engineering, Tel-Aviv 69978, Israel.

This work was done while the author was a National Research Council - NASA Research Associate at NASA Lewis Research Center. Work funded under NASA Grant NAGW-2022.

## 1. INTRODUCTION

Mission to Martian surface will require electric power. A power supply that requires little installation time, being light weight and stowed in a small volume can be accomplished by a photovoltaic (PV) array. A tent-shaped structure with a flexible PV blanket for solar power generation is proposed in [1], Fig. 1. The array is designed with a self-deploying mechanism using a pressurized gas expansion. The structural design for the array uses a combination of cables, beams and columns to support and deploy the PV blanket. The array is stowed with the blanket either folded or rolled. The main contribution to the stress in the structure is due to the tension in the cable which supports the PV blanket. The shape of the PV blanket is determined by an optimization between reduction in the cable tension and increase in blanket area. Under the force of gravity a cable carrying a uniformly distributed load will take the shape of a catenary curve,  $f_c(y)$ , with respect to the Y-Z plane, Fig. 2.

According to [2] and with some manipulations,  $f_c(y)$  is given by:

$$f_c(y) = k \left[ \cosh\left(\frac{D - y}{k}\right) - 1 \right] \quad (1)$$

The catenary constant  $k$  can be determined using the condition  $f_c(0) = H$  and solving iteratively. However, when the blanket is fairly taut, the load may be assumed uniformly distributed along the y-axis and the catenary curve may be approximated by a parabola [2], i.e.,:

$$f_c(y) = \frac{H}{D^2} (D - y)^2 \quad (2)$$

which simplifies the calculation.

Because of the shape of a catenary-tent-collector, a self-shading effect occurs on one of its sides (side B in Fig. 2). In this article we analyze the shadow shape and area. Based on these results, the beam insolation on the collector is calculated. We also determine the diffuse and the albedo insolation on the collector. An example for the planet Mars is given for the location of Viking Lander 1. Results for the parabolic approximation is given in Appendix B.

## 2. SHADOW CALCULATION

The catenary-tent-collector is self shading. The size of the shadow and the side which is shaded depend on the sun position. In general, both sides of the collector will be alternately shaded in a given day if at sunrise

$$\gamma_{sr} < \gamma_c - 90^\circ \quad (3)$$

where

$\gamma_c$  - the collector azimuth

$\gamma_{sr}$  - the sun azimuth at sunrise.

The azimuth angles are measured from true south positively in a clockwise direction. In days when eq. (3) is not satisfied, only one side of the collector is shaded all the times. In this paper we analyze the shape and size of the shadow cast on a catenary-tent-collector facing the south-north direction. The results can be generalized for an arbitrary oriented tent by replacing the sun azimuth angle  $\gamma_s$  by the difference between the solar and the collector

azimuth angles, i.e.,

$$\gamma = \gamma_s - \gamma_c \quad (4)$$

With reference to Fig. 3, the shadow cast by line  $\overline{ON}$  can be divided into three distinct cases:

- (i)  $P_x < L$  ,  $P_y < D$
- (ii)  $P_x < L$  ,  $P_y \geq D$  (5)
- (iii)  $P_x \geq L$  ,  $P_y < D$

It will be shown later that for the case  $P_x \geq L$ ,  $P_y \geq D$  the shadow takes the shape either of case (ii) or case (iii).

The components  $P_x$  and  $P_y$  of the line  $\overline{OP}$  was derived in [3,4] and are:

$$P_x = H \cos \delta \sin \omega / \sin \alpha \quad (6)$$

and

$$P_y = H(\sin \phi \cos \delta \cos \omega - \cos \phi \sin \delta) / \sin \alpha \quad (7)$$

where

$$\sin \alpha = \sin \phi \sin \delta + \cos \phi \cos \delta \cos \omega \quad (8)$$

and

$\delta$  - solar declination angle

$\phi$  - local latitude

$\alpha$  - sun elevation angle

$\omega$  - solar hour angle

Case (i):  $P_x < L$ ,  $P_y < D$

In this case the solar rays penetrate the collector surface and the shadow on the collector takes the shape NTEE<sub>x</sub>M as shown in Fig. 4. Point E is a point where the ray penetrates the collector, and point T is a point where the ray is tangent to the collector. In order to calculate the shaded area, the components of the points E and T must be determined. Since the catenary function  $f_c(y)$  is hyperbolic, the solution for the component  $y_E$  is obtained numerically from the solution of the following equation (see Appendix A):

$$\frac{k}{H} \cosh\left(\frac{D - y_E}{k}\right) + \frac{y_E}{P_y} = 1 + \frac{k}{H} \quad (9)$$

The component  $x_E$  is then given by (see Fig. 4)

$$x_E = \frac{P_x}{P_y} y_E \quad (10)$$

Point T is in y-z plane, i.e.,  $x_T = 0$  and  $y_T$  is obtained from the solution of (see Appendix A):

$$y_T = D - k \sinh^{-1}(H/P_y) \quad (11)$$

It is easier to obtain the shaded area  $A_{sh}$  from the "stretched out" collector, Fig. 4(b), i.e.,

$$A_{sh} = \widehat{L N E_y} - 0.5 x_E \widehat{T E_y} \quad (12)$$

The unshaded area  $A_{ush}$  is given by:

$$A_{ush} = A - A_{sh} = L(\widehat{N N_n} - \widehat{N E_y}) + 0.5 x_E \widehat{T E_y} \quad (13)$$

where  $A$  is the area of one side of the collector, i.e.,

$$A = L \widehat{N N_n} \quad (14)$$

Defining a relative shaded area by  $\xi$ , we obtain

$$\xi = (2 L \widehat{N E_y} - x_E \widehat{T E_y}) / 2L \widehat{N N_n} \quad (15)$$

The length of an arc between two points  $y_1$  and  $y_2$  is given by:

$$\widehat{y_1 y_2} = \int_{y_1}^{y_2} \sqrt{1 + [f_c'(y)]^2} dy \quad (16)$$

where  $f_c'(y)$  is the derivative of the function  $f_c(y)$ . The length of the arcs in eq. (15) thus become:

$$\widehat{N N_n} = \int_0^D \sqrt{1 + [f_c'(y)]^2} dy = k \sinh(D/k) \quad (17)$$

$$\widehat{N E_y} = \int_0^{y_E} \sqrt{1 + [f_c'(y)]^2} dy = k \left[ \sinh(D/k) + \sinh\left(\frac{y_E - D}{k}\right) \right] \quad (18)$$

$$\widehat{T E_y} = \int_{y_T}^{y_E} \sqrt{1 + f_c'(y)^2} dy = k \left[ \sinh\left(\frac{y_E - D}{k}\right) + \sinh\left(\frac{D - y_T}{k}\right) \right] \quad (19)$$

Case (ii):  $P_x < L$  ,  $P_y \geq D$

This case is shown in Fig. 5. The array touches the collector at the foot, point E, and at point U. The coordinates of point E are:

$$y_E = D \quad (20)$$

As derived in Appendix A,



$$x_E = \frac{P_x}{P_y} (D - y_U) \quad (21)$$

where  $y_U$  is determined from the solution of (see Appendix A):

$$k \left[ \cosh\left(\frac{D - y_U}{k}\right) - 1 \right] + \frac{H}{P_y} y_U = \frac{DH}{P_y} \quad (22)$$

The coordinates of point T are the same as for case (i), i.e.,  $x_T = 0$  and  $y_T$  is given by eq. (11). The shaded and unshaded areas, Fig. 5(b), are, respectively:

$$A_{sh} = A - 0.5 x_E \widehat{T N_n} \quad (23)$$

$$A_{ush} = 0.5 x_E \widehat{T N_n} \quad (24)$$

The relative shaded area is obtained as:

$$\xi = 1 - \frac{x_E \widehat{T N_n}}{2 L N_n} \quad (25)$$

where the arc length  $\widehat{T N_n}$  is given by:

$$\widehat{T N_n} = \int_{y_T}^D \sqrt{1 + [f_c'(y)]^2} dy = k \sinh\left(\frac{D - y_T}{k}\right) \quad (26)$$

and  $N_n$  is given in eq. (17).

Case (iii):  $P_x > L$ ,  $P_y < D$

The solar ray may either intersect the collector or may fall outside the collector. The case of intersection was already analysed in case (i). To determine whether the solar ray intersects the collector, eqs. (9) and (10) are solved.

If  $x_E < L$  than there is an intersection. If  $x_E > L$  than there is no intersection, see Fig. 6. The coordinates of point E are:

$$x_E = L \quad (27)$$

and  $y_E$  is determined from the solution of (see Appendix A):

$$k \left[ \cosh \left( \frac{D - y_E + L \frac{P_x}{P_y}}{k} \right) - \cosh \left( \frac{D - y_E}{k} \right) \right] = \frac{L H}{P_x} \quad (28)$$

The coordinates of point T are  $x_T = 0$  and  $y_T$  is given by eq. (11). The shaded and unshaded areas, Fig. 6, are respectively:

$$A_{sh} = L \widehat{N E_y} - 0.5 L \widehat{T E_y} \quad (29)$$

$$A_{ush} = L(\widehat{N N_n} - \widehat{N E_y} + 0.5 \widehat{T E_y}) \quad (30)$$

The relative shaded area is:

$$\xi = (2 \widehat{N E_y} - \widehat{T E_y}) / 2 \widehat{N N_n} \quad (31)$$

where  $\widehat{N N_n}$ ,  $\widehat{N E_y}$  and  $\widehat{T E_y}$  are given in eqs. (17)-(19).

The case  $P_x \geq L$ ,  $P_y \geq D$  corresponds either to case (ii) or to case (iii) depending on the ratio  $P_x/P_y$  of the ray  $\overline{OP}$  (see Fig. 7).

For  $P_x/P_y < L/D$  the solution is as for case (ii) and

for  $P_x/P_y \geq L/D$  the solution is as for case (iii)

For a south-north oriented collector, the shadow as a function of time is symmetrical with the solar noon. For the after noon, the shadow calculations are with respect to line O'M (see Fig. 3).

### 3. SOLAR RADIATION CALCULATION

With the results developed in the previous section, the beam irradiance in W or W/m<sup>2</sup> and the beam insolation in Whr/day or Whr/m<sup>2</sup>-day on the catenary-tent-collector can be determined. The diffuse and albedo components will be added to the beam to get the global irradiance and insolation. A north-south facing catenary-tent-collector will be considered. A generalization to any arbitrary oriented tent may be obtained using eq. (4).

#### Beam Irradiance

The beam irradiance on both sides of the tent depends on the self-shading condition of eq. (3). In calculating the irradiance on an unshaded side we resort to Fig. 8. The beam irradiance  $P$ , in watts (W), on an unshaded side is given by:

$$dP_b = G_b \cos\theta \, dA \quad (32)$$

where  $G_b$  is the beam irradiance in W/m<sup>2</sup> normal to the solar rays, and  $\theta$  is the angle between the solar rays and the normal to the surface.  $\cos\theta$  and  $dA$  are given by

$$\cos\theta = \cos\beta(y) \sin\alpha + \sin\beta(y) \cos\alpha \cos\gamma_s \quad (33)$$

and

$$dA = L \, dS = L \sqrt{1 + [f_c'(y)]^2} \, dy \quad (34)$$

where  $dS$  is the unit length of the collector (Fig. 8) and

$$\sin\beta(y) = |f_c'(y)| / \sqrt{1 + [f_c'(y)]^2} \quad (35)$$

$$\cos\beta(y) = 1 / \sqrt{1 + [f_c'(y)]^2} \quad (36)$$

Therefore, eq. (32) reduces to:

$$dP_b = G_b L(\sin\alpha + |f_c'(y)| \cos\alpha \cos\gamma_s) dy \quad (37)$$

Integrating eq. (37) in the interval  $[0, D]$ , we obtain the beam irradiance, in  $W$ , on the unshaded side of the collector, i.e.,

$$P_b = G_b L(D \sin\alpha + H \cos\alpha \cos\gamma_s) \quad (38)$$

Using the angle  $\epsilon$  as defined in Fig. 8, we obtain:

$$P_b = G_b L(H^2 + D^2)^{1/2} (\cos\epsilon \sin\alpha + \sin\epsilon \cos\alpha \cos\gamma_s) \quad (39)$$

i.e., the beam irradiance on a catenary collector is equivalent to that of a flat plate collector  $MNM_s N_s$ . This conclusion is also valid for any non-flat shape collector.

The beam irradiance on a collector that is partially shaded can not be obtained by multiplying the incoming beam irradiance with the factor  $(1-\xi)$  as for a flat plate collector since the beam irradiance on the collector is not uniform along the  $y$  axis of the collector, i.e., the angle  $\theta$  varies with  $y$ . Using eqs. (33), (35) and (36), the variation of the beam irradiance, in  $W/m^2$ , along the collector is:

$$G_b(y) = \frac{G_b}{\sqrt{1 + [f_c'(y)]^2}} [\sin\alpha + \cos\alpha \cos\gamma_s |f_c'(y)|]$$

and with eq. (1) we obtain:

$$G_b(y) = \frac{G_b}{\cosh\left(\frac{D-y}{k}\right)} \left[ \sin\alpha + \cos\alpha \cos\gamma_s \left| \sinh\left(\frac{D-y}{k}\right) \right| \right] \quad (40)$$

With reference to Fig. 9(a), the beam irradiance on the partially shaded side of the

collector for case (i) is given by:

$$P_b^{sh} = \int_{y_T}^{y_E} G_b(y) dA_1 + \int_{y_E}^D G_b(y) dA_2$$

where  $G_b(y)$  is given by eq. (40), and

$$dA_1 = x dS = x \cosh\left(\frac{D-y}{k}\right) dy \quad (41)$$

$$dA_2 = L \cosh\left(\frac{D-y}{k}\right) dy \quad (42)$$

where  $x$  and  $y$  are related by (Fig. 9(a))

$$x = \left(\frac{x_E}{y_E - y_T}\right)(y - y_T) \quad (43)$$

Substituting these results, we obtain the beam irradiance on the partially shaded side of the collector:

$$\begin{aligned} P_b^{sh} = G_b \left\{ \int_{y_T}^{y_E} \left[ \sin\alpha + \cos\alpha \cos\gamma_s \left| \sinh\left(\frac{D-y}{k}\right) \right| \right] \left( \frac{x_E}{y_E - y_T} \right) (y - y_T) dy \right. \\ \left. + L \int_{y_E}^D \left[ \sin\alpha + \cos\alpha \cos\gamma_s \left| \sinh\left(\frac{D-y}{k}\right) \right| \right] dy \right\} \quad (45) \end{aligned}$$

Similarly, the beam irradiance for case (ii) (Fig. 9b) is:

$$P_b^{sh} = G_b \int_{y_T}^D \left[ \sin\alpha + \cos\alpha \cos\gamma_s \left| \sinh\left(\frac{D-y}{k}\right) \right| \right] \left( \frac{x_E}{D - y_T} \right) (y - y_T) dy \quad (46)$$

and the beam irradiance for case (iii) (Fig. 9c) is:

$$P_b^{sh} = G_b \left\{ \int_{y_T}^{y_E} \left[ \sin\alpha + \cos\alpha \cos\gamma_s \left| \sinh\left(\frac{D-y}{k}\right) \right| \right] \left( \frac{L}{y_E - y_T} \right) (y - y_T) dy \right. \\ \left. + L \int_{y_E}^D \left[ \sin\alpha + \cos\alpha \cos\gamma_s \left| \sinh\left(\frac{D-y}{k}\right) \right| \right] dy \right\} \quad (47)$$

In winter, side A (Fig. 2) remains always unshaded, therefore the beam irradiance  $P_{bA}$  on this side is given by eq. (38) or eq. (39). Side B may be partially shaded and the beam irradiance  $P_{bB}^{sh}$  is given by eqs. (45), (46) or (47) where the collector azimuth is  $180^\circ$ , therefore,  $\gamma_s$  is replaced by  $(\gamma_s - 180^\circ)$ . The total beam irradiance on the catenary-tent-collector in winter is:

$$P_b = P_{bA} + P_{bB}^{sh} \quad (48)$$

In summer, early in the morning and late in the afternoon, side A is partially shaded, therefore, the beam irradiance  $P_{bA}$  is given by eqs. (45), (46) or (47). Side B is unshaded, and the beam irradiance  $P_{bB}$  is given by eq. (38) with the azimuth  $\gamma_s - 180^\circ$ , i.e.,

$$P_{bB} = G_b L [D \sin\alpha + H \cos\alpha \cos(\gamma_s - 180^\circ)] \quad (49)$$

thus the beam irradiance on both sides of the tent collector for early morning and late afternoon hours is:

$$P_b = P_{bA}^{sh} + P_{bB} \quad (50)$$

For other hours of the day, side B will be partially shaded and eq. (48) applies.

### Diffuse Irradiance

The diffuse irradiance on an incremental area  $dA$  is given by

$$dP_d = G_{dh} dA F_{dA-S} \quad (51)$$

where

$G_{dh}$  - diffuse irradiance on a horizontal surface

$F_{dA-S}$  - view factor of  $dA$  with respect to the sky

For sufficiently small  $dS$ , the view factor for  $dA$  is given by:

$$F_{dA-S} = 0.5[1 + \cos\beta(y)] \quad (52)$$

Using eqs. (34), (36) and (52) for eq. (51) we obtain:

$$dP_d = 0.5 G_{dh} L(\sqrt{1 + [f_c'(y)]^2} + 1)dy$$

Integrating for  $y$  in the interval  $[0, D]$  we get the diffuse irradiance on one side of the tent:

$$P_d = 0.5 G_{dh} L(\widehat{N N_n} + D) = 0.5 G_{dh} L[k \sinh(D/k) + D] \quad (53)$$

Since the diffuse irradiance is independent of the orientation of the collector (for isotropic skies), eq. (53) applies also to the other side of the tent.

The view factor of a catenary collectors can now be calculated by defining:

$$P_d = G_{dh} A F_{A-S} \quad (54)$$

using eqs. (17) and (53) one obtains:

$$F_{A-S} = 0.5 \left[ 1 + \frac{D}{k \sinh(D/k)} \right] \quad (55)$$

### Albedo

The albedo can be determined by using the expression:

$$P_{al} = a_l G_h A F_{A-G} \quad (56)$$

where  $a_l$  - the albedo factor

$G_h$  - global irradiance on a horizontal surface

$F_{A-G}$  - view factor of area  $A$  with respect to ground

The view factor of area  $A$  with respect to the sky,  $F_{A-S}$ , and with respect to the ground,  $F_{A-G}$ , are related by [5]:

$$F_{A-S} + F_{A-G} = 1 \quad (57)$$

obtaining with eq. (55):

$$F_{A-G} = 0.5 \left[ 1 - \frac{D}{k \sinh(D/k)} \right] \quad (58)$$

Using eq. (14), (17), (56) and (58) we obtain the albedo irradiance on one side of the tent as:

$$P_{al} = 0.5 a_l G_h L [k \sinh(D/k) - D] \quad (59)$$

Since the albedo irradiance is independent on the orientation of the collector eq. (59) applies also to other side of the tent.

## 4. Example

The example refers to a south-north facing catenary-tent-collector deployed on the Mars surface [6] at the locations of Viking Lander VLI (Latitude - 22.3°N, Longitude -



47.9°W) and in an autumn day  $L_s = 200^\circ$  [6]. For this time of the year eq. (3) does not apply and, therefore, only side B will be partially shaded during the day. The dimensions of the catenary collector are:  $D = 3\text{m}$ ,  $H = 2\text{m}$  and  $L = 1.5\text{m}$ . Since  $f_c(0) = H$ , this results in  $k = 2.53$  and the catenary equation is given by:

$$f_c(y) = 2.53[\cosh(1.186 - 0.395y) - 1] \quad (60)$$

Figure 10(a) shows the shadow shapes on side B of the catenary collector for  $\phi = 22.3^\circ\text{N}$  for different hours of the day. The shadow calculations are based on section 2. For comparison, the shadow shapes for  $\phi=32^\circ$  are shown in Fig. 10(b). As expected, the self-shading effect is more pronounced for higher latitudes. It is interesting to note that for  $\phi=22.3^\circ\text{N}$ , the shadow effect is quite small during the noon hours. In summer, the shadow will be even less.

The insolation of the catenary-tent-collector for  $\phi=22.3^\circ\text{N}$ ,  $L_s=200^\circ$  and albedo  $al=0.22$  is shown in Table 1 based on radiation data at VLI [6]. The table shows the beam, diffuse and the albedo insulations on sides A and B in kWhr-day and kWhr/m<sup>2</sup>-day. As expected, the beam insolation on side B is lower by 59.6% than on side A. It is interesting to note that the diffuse insolation comprises 46.6% of the global insolation. This characteristic is typical for Mars, a place where the atmosphere consists mainly of dust particles.

Table 1. - Insolation on a catenary-tent collector,  $\phi=22.3^\circ\text{N}$ ,  $L_s=200^\circ$ ,  $al=0.22$

	BEAM COMPONENT			DIFFUSE COMPONENT	ALBEDO COMPONENT	GLOBAL INSOLATION
	side A	side B	Total			
Q(kWhr-day)	12.65	5.11	17.76	16.27	0.89	34.92
q(kWhr/m <sup>2</sup> -day)	2.246	0.907	1.577	1.445	0.079	3.101

## 5. CONCLUSIONS

The article analyses the performance of a catenary-tent-collector [1] (a flexible blanket that falls freely on both sides of a central support). This kind of collectors has characteristics (portability and simplicity) that are desirable for solar power plants on outer space planets. Because of its shape, there is a self-shading effect that must be taken into account in the solar radiation calculation. Therefore, the shape and area of the shadow on the collector is calculated and used in the determination of the beam radiation. The diffuse and albedo radiation were also calculated to determine the global radiation on the collector. The numerical example is based on solar radiation data on Mars.

## 6. NOMENCLATURE

$A$	Collector area, [m <sup>2</sup> ]
$A_{sh}$	shaded area of a collector, [m <sup>2</sup> ]
$A_{ush}$	unshaded area of a collector, [m]
$D$	length of the collector, [m]
$F_{A-G}$	view factor of area $A$ with respect to ground
$F_{A-S}$	view factor of area $A$ with respect to sky
$F_{dA-S}$	view factor of incremental area $dA$ with respect to sky
$G_b$	direct beam irradiance, [W/m <sup>2</sup> ]
$G_{dh}$	diffuse irradiance on a horizontal surface, [W/m <sup>2</sup> ]
$G_h$	global irradiance on a horizontal surface, [W/m <sup>2</sup> ]
$H$	height of collector, [m]
$k$	catenary constant

$L$	collector width, [m]
$L_s$	areocentric longitude of the sun (for Mars)
$P_{al}$	albedo irradiance, [W]
$P_b$	direct beam irradiance on an unshaded side of a collector, [W]
$P_b^{sh}$	direct beam irradiance on a partially shaded side of a collector, [W]
$P_{bA}, P_{bB}$	direct beam irradiance on an unshaded side A and B of a collector, respectively, [W]
$P_{bA}^{sh}, P_{bB}^{sh}$	direct beam irradiance on a partially shaded side A and B of a collector, respectively, [W]
$P_x, P_y$	x and y components of a shadow length, [m]
$Q$	insolation, [kWhr-day]
$q$	insolation, [kWhr/m <sup>2</sup> -day]
$\alpha$	sun altitude
$\gamma_c$	collector azimuth
$\gamma_s$	sun azimuth
$\gamma_{sr}$	sun azimuth at sunrise
$\delta$	solar declination angle
$\epsilon$	characteristic angle of the collector
$\theta$	angle between solar ray and the normal to the collector
$\xi$	relative shaded area
$\phi$	local latitude
$\omega$	solar hour angle

## 7. REFERENCES

- [1] A.J. Colozza, "Design, Optimization, and Analysis of a Self-Deploying PV Tent Array", NASA Contract Report 187119, June 1991.
- [2] F.B. Beer, E.R. Johnston, Mechanical for Engineers: Static and Dynamics McGraw-Hill, New York, 1967, pp. 258-273.
- [3] J. Appelbaum, J. Bany, "Shadow Effect of Adjacent Solar Collectors in Large Scale Systems" Solar Energy, Vol. 23, pp. 497-507, 1979.
- [4] J. Bany, J. Appelbaum "The Effect of Shadowing on the Design of Field of Solar Collectors" Solar Cell, Vol. 20, pp. 201-228, 1987.
- [5] H.C. Hottel, A.F. Sarofim, Radiative Transfer, McGraw Hill, New York, 1967, pp. 25-39.
- [6] J. Appelbaum D.J. Flood, "Solar Radiation on Mars", Solar Energy, Vol. 45, pp. 353-363, 1990.

## APPENDIX A

### Calculation of points E and T

#### Calculation of Point E and T for case (i)

##### Point E

Point E may be calculated from the projection of the solar ray  $\overline{NP}$  on the z-y plane, Fig. A1 (a). The projection line equation is:

$$z = H(1 - y/P_y) \quad (A.1)$$

The intersection of the projection line, eq. (A1) with the catenary equation  $f_c(y)$  yields the coordinate  $y_E$ , i.e., the solution of:

$$\frac{k}{H} \cosh\left(\frac{D - y_E}{k}\right) + \frac{y_E}{P_y} = 1 + \frac{k}{H} \quad (A.2)$$

The coordinate  $x_E$  is on line  $\overline{OP}$ , i.e.,

$$x_E = \frac{P_x}{P_y} y_E \quad (A.3)$$

and finally the coordinate  $z_E$  is calculated from eq. (A1).

##### Point T

Point T is determined by a sun ray that its projection on the z-y plane is tangent to the arc  $\widehat{N N_n}$ , Fig. A1 (b), i.e., at this point, the derivative of  $f_c(y)$  is equal to the slope of line  $\overline{AB}$ . From eq. (1)

$$f_c'(y) = -\sinh\left(\frac{D - y}{k}\right) \quad (A.4)$$

Since  $\overline{AB}$  and  $\overline{N P_y}$  are parallel lines, the slope of line  $\overline{AB}$  is  $-H/P_y$ , thus obtaining:

$$y_T = D - k \sinh^{-1}(H/P_y) \quad (\text{A.5})$$

The coordinate  $x_T = 0$  and the coordinate  $z_T$  is calculated from the  $f_c(y)$  equation.

Calculation of  $y_U$  and  $x_E$  for case (ii)

A sun ray that touches the foot of the tent at point E passes through point U on the blanket, Figs. 5 and A.1.(a). It follows that

$$(D - y_U)/x_E = P_y/P_x \quad (\text{A.6})$$

and

$$\frac{z_U}{D - y_U} = \frac{f_c(y_U)}{D - y_U} = \frac{H}{P_y} \quad (\text{A.7})$$

from which  $y_U$  is determined by solving:

$$f_c(y_U) + \frac{H}{P_y} y_U = \frac{DH}{P_y} \quad (\text{A.8})$$

where  $f_c(y)$  is given in eq. (1). The coordinate  $x_E$  is then calculated from eq. (A.6).

Calculation of  $y_E$  for case (iii)

Referring to Figs. 6 and A.1 (b), we may write

$$(y_E - y_U)/L = P_y/P_x \quad (\text{A.9})$$

and

$$\frac{z_U - z_E}{y_E - y_U} = \frac{f_c(y_U) - f_c(y_E)}{y_E - y_U} = \frac{H}{P_y} \quad (\text{A.10})$$

From eqs. (A.9) and (A.10),  $y_E$  is determined by:

$$f_c\left(y_E - L \frac{P_y}{P_x}\right) - f_c(y_E) = \frac{L H}{P_x} \quad (\text{A.11})$$

where  $f_c(y)$  is given in eq. (1).

## APPENDIX B

Using the parabolic approximation for  $f_c(y)$  greatly simplifies the mathematical calculation. The error is small and the results are very similar to the catenary case. The procedure for calculating the points for the shadows are the same as in Appendix A but now  $f_c(y)$  is the parabolic approximation (eq. (2)), i.e.,

$$f_c(y) = H\left(1 - \frac{y}{D}\right)^2, \quad f_c'(y) = \frac{-2H}{D} \left(1 - \frac{y}{D}\right) \quad (\text{B.1})$$

### Case (i)

The coordinates of points E and T are:

$$x_E = D \cdot \frac{P_x}{P_y} \left(2 - \frac{D}{P_y}\right), \quad y_E = D \left(2 - \frac{D}{P_y}\right), \quad z_E = H \left(\frac{D}{P_y} - 1\right)^2 \quad (\text{B.2})$$

$$x_T = 0, \quad y_T = D \left(1 - \frac{D}{2P_y}\right), \quad z_T = H \left(\frac{D}{2P_y}\right)^2 \quad (\text{B.3})$$

With these results, the arcs  $\widehat{N N_n}$ ,  $\widehat{N E_y}$  and  $\widehat{T E_y}$  can now be determined. The length of an arc is given by eq. (16) and for the parabolic approximation we have:

$$g(y) = \int \sqrt{1 + [f_c'(y)]^2} dy = \int \sqrt{1 + \left[\frac{2H}{D^2} (D - y)\right]^2} dy$$

the solution of the integral is:

$$g(y) = \frac{D^2}{4H} \sinh^{-1} \left[ \frac{2H}{D^2} (y - D) \right] + \frac{1}{2}(y - D) \sqrt{1 + \left[ \frac{2H}{D^2} (y - D) \right]^2} \quad (B.4)$$

The arc lengths are therefore:

$$\widehat{N N_n} = g(D) - g(0) \quad (B.5)$$

$$\widehat{N E_y} = g(y_E) - g(0) \quad (B.6)$$

$$\widehat{T E_y} = g(y_E) - g(y_T) \quad (B.7)$$

Case (ii)

Solving eq. (A.8) with eq. (2) for  $y_U$  (Fig. 5) results in:

$$y_U = D \left( 1 - \frac{D}{P_y} \right) \quad (B.8)$$

and using eq. (A.6) we obtain the coordinates of  $x_E$ . The coordinates of points E and T are:

$$x_E = P_x \left( \frac{D}{P_y} \right)^2, \quad y_E = D, \quad z_E = 0 \quad (B.9)$$

$$x_T = 0, \quad y_T = D \left( 1 - \frac{D}{2P_y} \right), \quad z_T = H \left( \frac{D}{2P_y} \right)^2 \quad (B.10)$$

The expression for  $\widehat{T N_n}$  is given by:

$$\widehat{T N_n} = g(y_T) - g(D) \quad (B.11)$$



where  $g(y)$  is given in eq. (4).

Case (iii)

Solving eq. (A.11) with eq. (2) for  $y_E$  (Fig. 6) results in:

$$y_E = D \left( 1 - \frac{D}{2P_y} \right) + L \frac{P_y}{2P_x} \quad (\text{B.12})$$

The coordinates of points E and T are:

$$x_E = L \quad , \quad y_E = D \left( 1 - \frac{D}{2P_y} \right) + L \frac{P_y}{2P_x} \quad , \quad z_E = H \left( \frac{D}{2P_y} - \frac{L P_y}{2DP_x} \right)^2$$

$$x_T = 0 \quad , \quad y_T = D \left( 1 - \frac{D}{2P_y} \right) \quad , \quad z_T = H \left( \frac{D}{2P_y} \right)^2$$

Table 1. - Insolation on a catenary-tent collector,  $\phi=22.3^\circ\text{N}$ ,  $L_s=200^\circ$ ,  $al=0.22$

	BEAM COMPONENT			DIFFUSE COMPONENT	ALBEDO COMPONENT	GLOBAL INSOLATION
	side A	side B	Total			
Q(kWhr-day)	12.65	5.11	17.76	16.27	0.89	34.92
q(kWhr/m <sup>2</sup> -day)	2.246	0.907	1.577	1.445	0.079	3.101

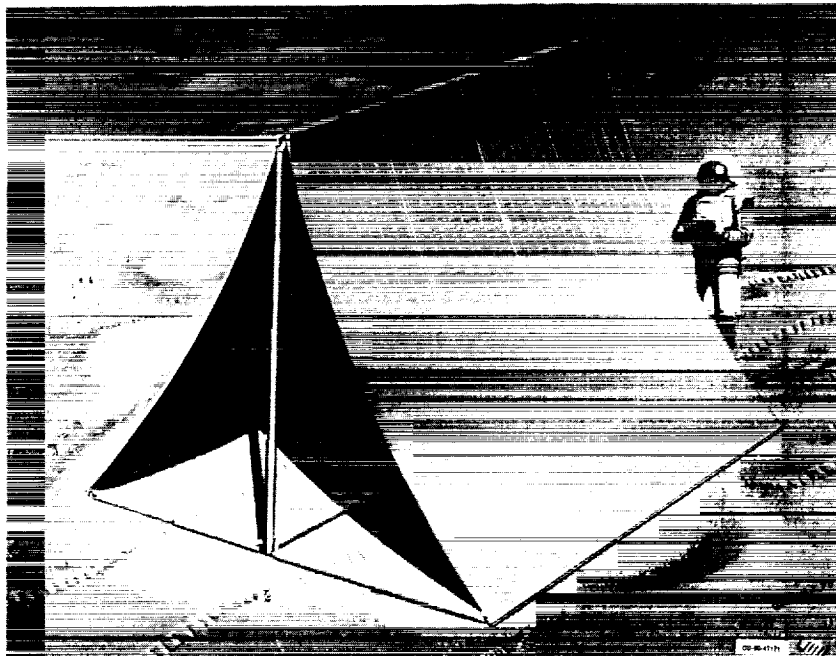


Figure 1.—Artist's view of a catenary-tent-collector.

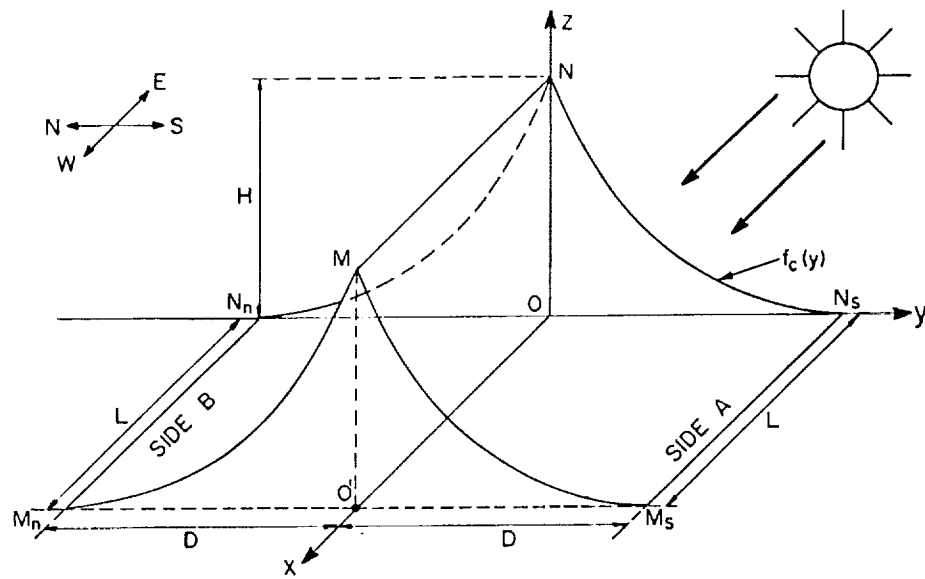


Figure 2.—Catenary-tent-collector: definitions and orientation.

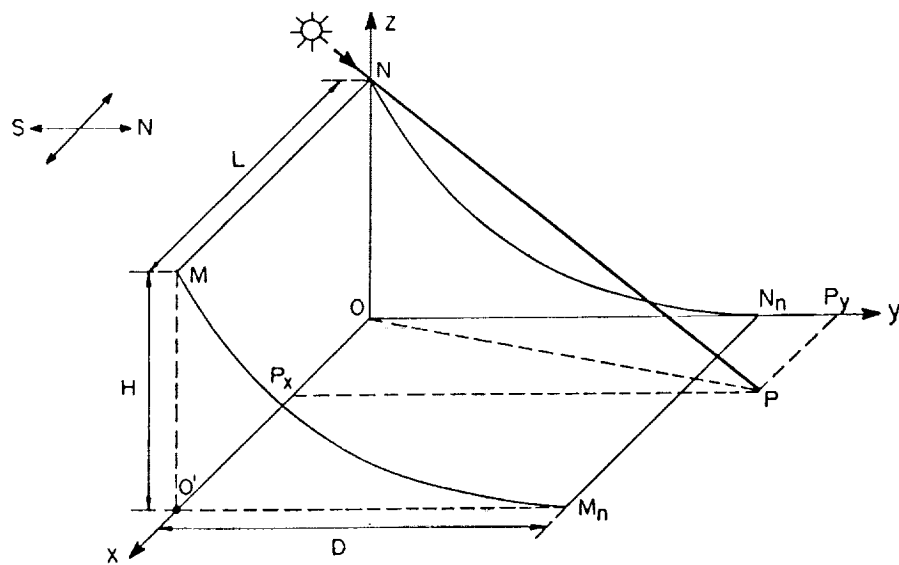


Figure 3.—Catenary collector: basic shadow parameters.

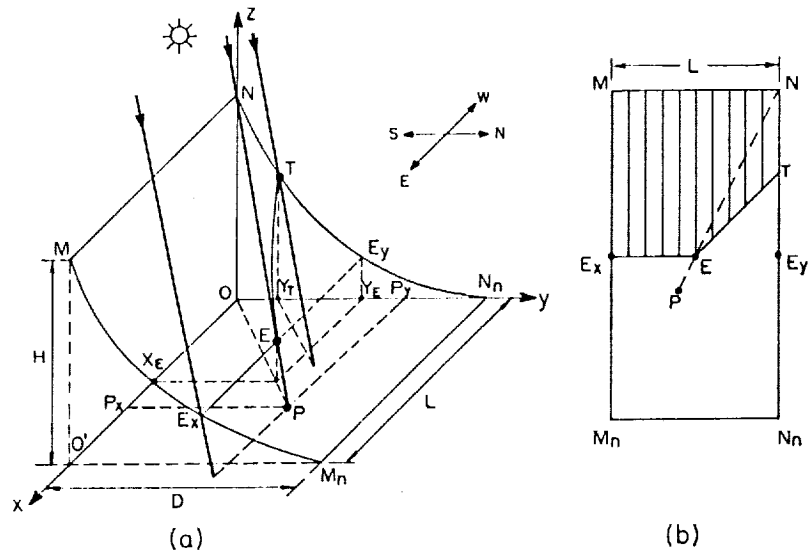


Figure 4.—Catenary collector - case (i) (a) shadow parameters, (b) stretched-out shadow shape.

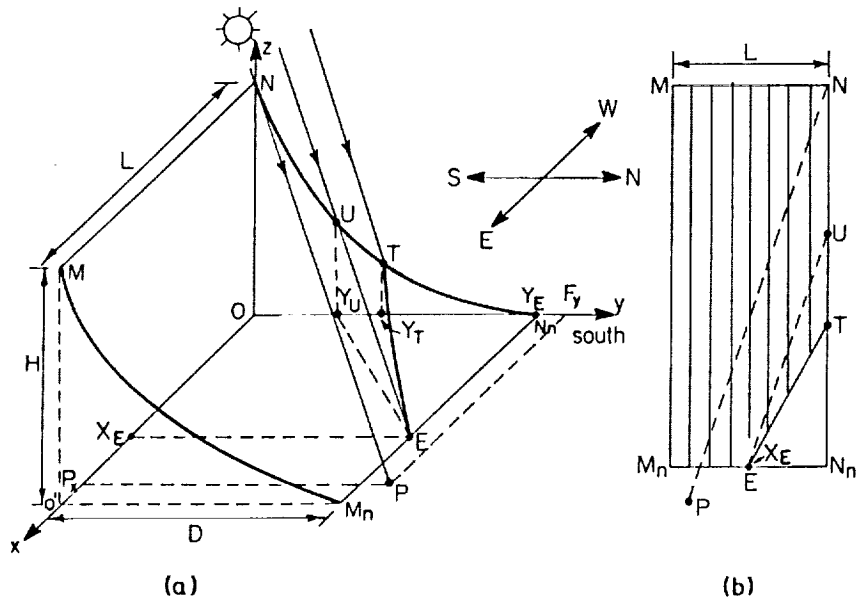


Figure 5.—Catenary collector - case (ii) (a) shadow parameters, (b) stretched-out shadow shape.

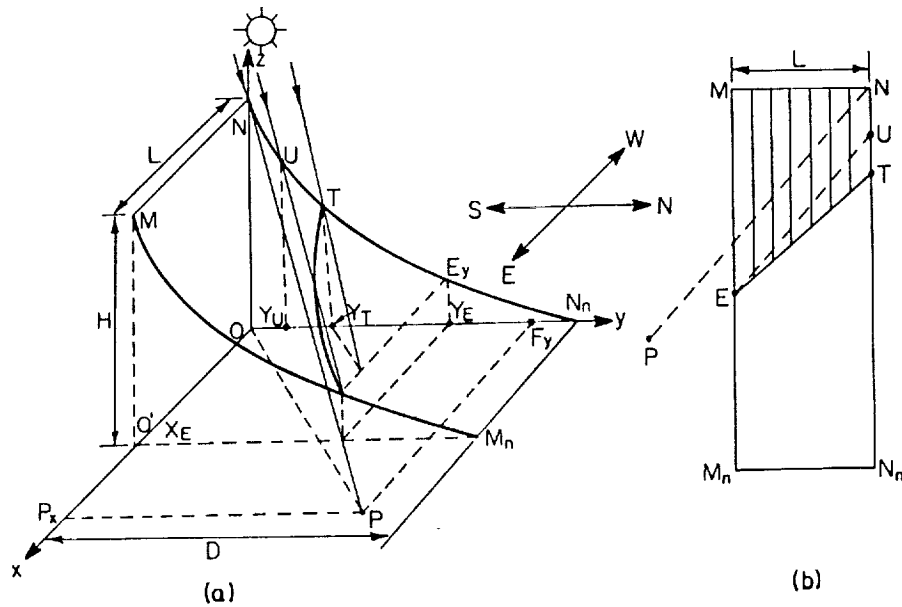


Figure 6.—Catenary collector - case (iii) (a) shadow parameters, (b) stretched-out shadow shape.

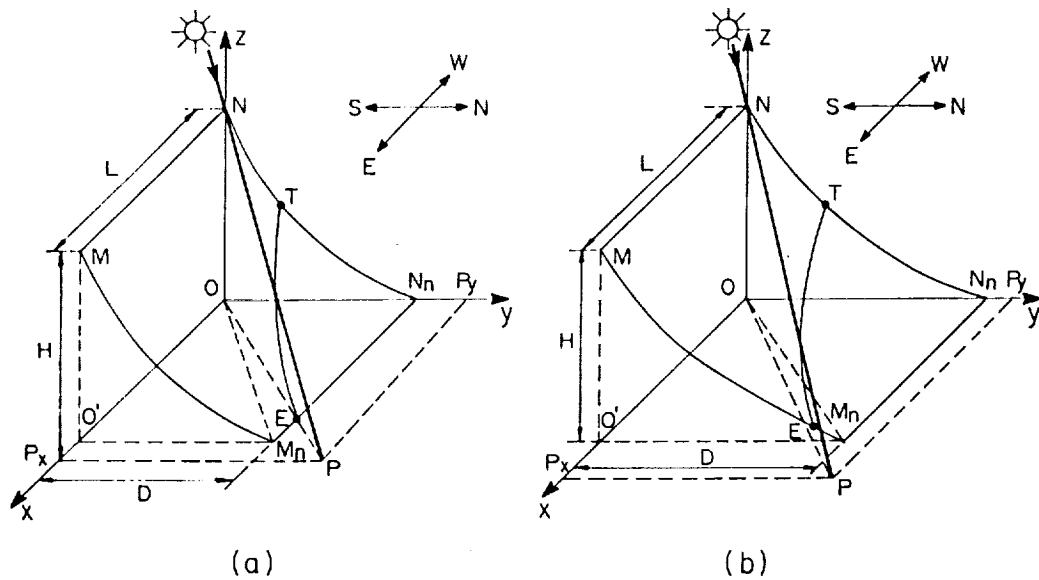


Figure 7.—Catenary collector - shadow shape for  $P_x \geq L$ ,  $P_y \geq D$  (a)  $P_x/P_y \geq L/D$ , (b)  $P_x/P_y < L/D$ .

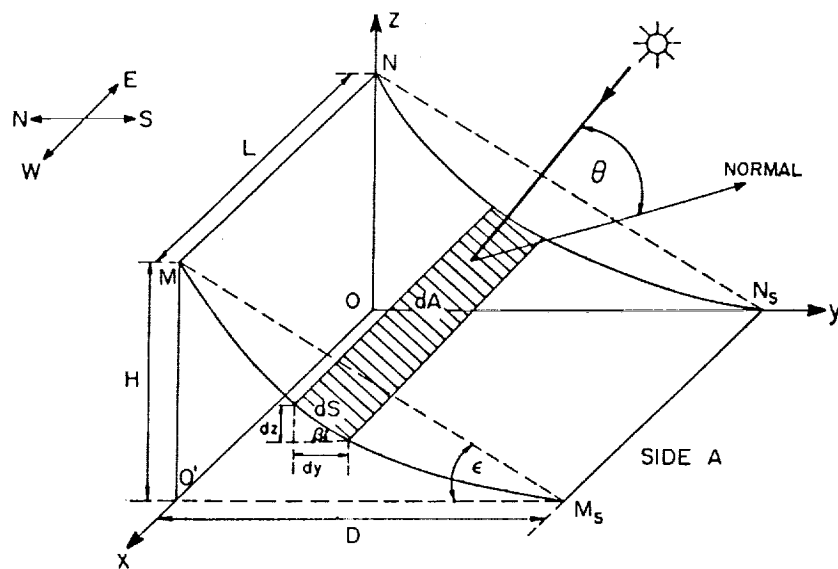
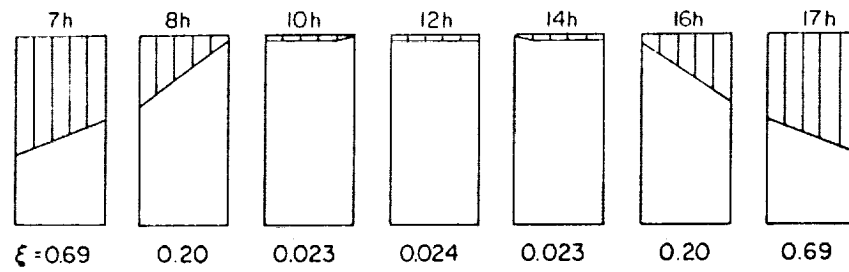
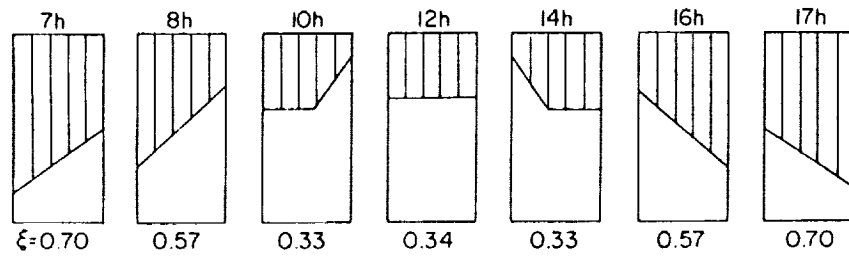


Figure 8.—Catenary collector - solar radiation calculation on an unshaded side.





(a)



(b)

Figure 10.—Catenary collector - shadow shapes on side B at different hours of the day for (a)  $\phi = 22.3^\circ\text{N}$ , (b)  $\phi = 32^\circ\text{N}$ .

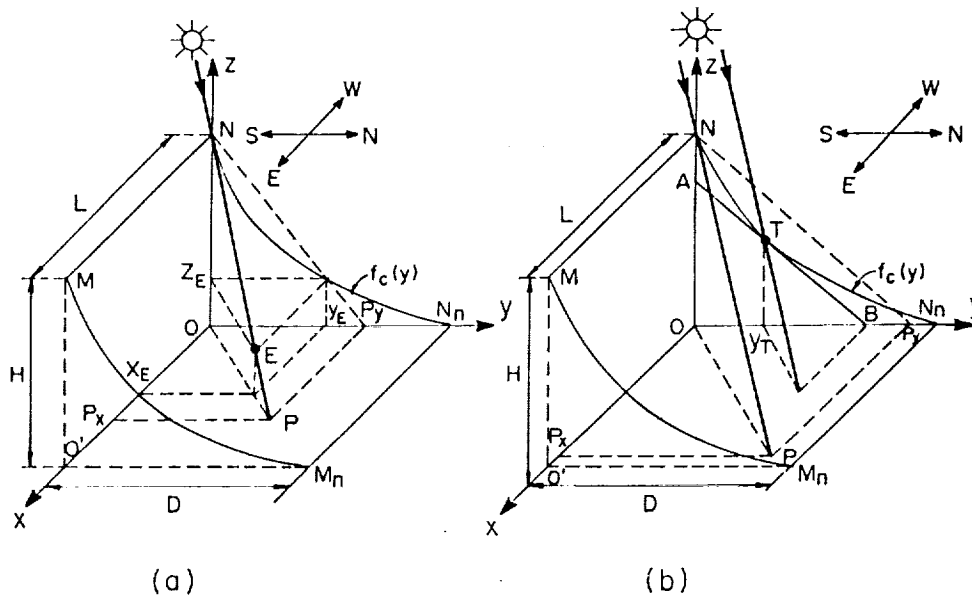


Figure A.1—Catenary collector - calculation of points (a) E, (b) T.





REPORT DOCUMENTATION PAGE			Form Approved OMB No. 0704-0188	
Public reporting burden for this collection of information is estimated to average 1 hour per response, including the time for reviewing instructions, searching existing data sources, gathering and maintaining the data needed, and completing and reviewing the collection of information. Send comments regarding this burden estimate or any other aspect of this collection of information, including suggestions for reducing this burden, to Washington Headquarters Services, Directorate for Information Operations and Reports, 1215 Jefferson Davis Highway, Suite 1204, Arlington, VA 22202-4302, and to the Office of Management and Budget, Paperwork Reduction Project (0704-0188), Washington, DC 20503.				
1. AGENCY USE ONLY (Leave blank)	2. REPORT DATE July 1992	3. REPORT TYPE AND DATES COVERED Technical Memorandum		
4. TITLE AND SUBTITLE Solar Radiation on a Catenary Collector		5. FUNDING NUMBERS  WU-506-41-11		
6. AUTHOR(S) M. Crutchik and J. Appelbaum				
7. PERFORMING ORGANIZATION NAME(S) AND ADDRESS(ES) National Aeronautics and Space Administration Lewis Research Center Cleveland, Ohio 44135-3191		8. PERFORMING ORGANIZATION REPORT NUMBER  E-7156		
9. SPONSORING/MONITORING AGENCY NAMES(S) AND ADDRESS(ES) National Aeronautics and Space Administration Washington, D.C. 20546-0001		10. SPONSORING/MONITORING AGENCY REPORT NUMBER  NASA TM-105751		
11. SUPPLEMENTARY NOTES M. Crutchik, Tel-Aviv University, Faculty of Engineering, Tel-Aviv 69978, Israel. J. Appelbaum, NASA Lewis Research Center, Cleveland, Ohio 44135.				
12a. DISTRIBUTION/AVAILABILITY STATEMENT  Unclassified - Unlimited Subject Category 33		12b. DISTRIBUTION CODE		
13. ABSTRACT (Maximum 200 words)  A tent-shaped structure with a flexible photovoltaic blanket acting as a catenary collector is presented. The shadow cast by one side of the collector on the other side producing a self shading effect is analyzed. The direct beam, the diffuse and the albedo radiation on the collector are determined. An example is given for the isolation on the collector operating on Mars surface for the location of Viking Lander 1 (VL1).				
14. SUBJECT TERMS Catenary collector; Flexible photovoltaic blanket; Solar radiation; Self shading; Shadow shape and size			15. NUMBER OF PAGES 32	
			16. PRICE CODE A03	
17. SECURITY CLASSIFICATION OF REPORT Unclassified	18. SECURITY CLASSIFICATION OF THIS PAGE Unclassified	19. SECURITY CLASSIFICATION OF ABSTRACT Unclassified	20. LIMITATION OF ABSTRACT	